The Iterative Self-Consistent Reaction-Field Method: The Refractive Index of Pure Water

KRISTIAN O. SYLVESTER-HVID,[1] KURT V. MIKKELSEN,[2] MARK A. RATNER[3]

[1]*Risø National Laboratory for Sustainable Energy, The Technical University of Denmark, DK-4000 Roskilde, Denmark*
[2]*Department of Chemistry, H. C. Ørsted Institute, University of Copenhagen, DK-2100 Copenhagen Ø, Denmark*
[3]*Department of Chemistry, Northwestern University, Evanston, IL 60208-3113*

Received 7 May 2010; accepted 24 June 2010
Published online 7 September 2010 in Wiley Online Library (wileyonlinelibrary.com).
DOI 10.1002/qua.22897

ABSTRACT: We present different microscopic models for describing electromagnetic properties of condensed phases and the models involve iterative self-consistent procedures for calculating the properties. We report calculations of the frequency-dependent refractive index of pure water. We investigate the importance of the first solvation shell and nonequilibrium solvent configurations, and present a procedure for estimating appropriate cavity sizes. © 2010 Wiley Periodicals, Inc. Int J Quantum Chem 111: 904–913, 2011

Key words: solvation; molecular properties; solvation shells

1. Introduction

The present contribution is concerned with ab initio continuum solvation models, applied in the description of pure liquid systems. These solvent models have become wide-spread in use because they afford reasonable estimates of solute properties as using simple representations of the solvent. Usually, the solvent is modelled as a linear, isotropic, and homogeneous dielectric medium, whereas the solute may be subject to almost any level of quantum theory available [1–36]. The coupling of the solvent and solute sub-systems is then treated based on the concepts of reaction field (RF) theory.

Improvements of continuum solvation models have left the basic RF concept surprisingly unchanged, relative to the efforts put into improving the description of the solute sub-system. Paramount to the latter is the electric representation of the solute charge distribution along with the underlying quantum mechanical method used to derive this. Hence,

Correspondence to: K. V. Mikkelsen; e-mail: kmi@kemi.ku.dk
Contract grant sponsors: NSF, ONR, Danish Natural Science Research Council, Danish Technical Research Council, Carlsberg Foundation, Danish Center for Scientific Computing, EU-Network NANOQUANT.

multipole expansion of the solute charge distribution to orders beyond dipole terms is necessary [15, 19, 27, 29, 37, 38], as is the use of correlated methods [13, 20, 21, 24, 39–55].

Much effort has gone into devising methods from which linear and nonlinear molecular optical properties can be obtained [25, 26, 29, 56–69], the interest being driven by the vast and growing area of experimental laser studies of solutions and liquids. Refinements in the representation of the surrounding medium have focused mainly on aspects such as the cavity geometry, radial dependence of the dielectric constant, and effects of inertial polarization [21, 23, 24, 27, 29]. Of these improvements, it seems that the last introduces the fewest additional parameters into the continuum solvation model.

In the refinement of the continuum RF model, we have previously addressed the issue of inertial solvent polarization in the context of deriving linear and nonlinear molecular optical properties. Thus, using the multiconfigurational self-consistent reaction field (MCSCRF) procedure [20], linear [21, 24], quadratic [41], and cubic [70] solvation response properties are computable, with (nonequilibrium) or without (equilibrium) consideration of inertial polarization effects.

Essential to the MCSCRF method is the assumption of infinite dilution, that is, the dielectric constant of the surrounding medium is unaffected by the presence of the solute. From an experimental point of view, such experiments can be intricate to realize which has motivated us to focus on the theoretical description of pure liquids as well [40]. Envisioning a pure liquid as a solute, solvated by identical molecules, is appealing but certainly violates the assumption of infinite dilution. The problem is the obvious methodological inconsistency, arising from modelling molecular optical properties for the constituents of a pure phase, using the dielectric constant as input, because this again is derived from the computed molecular optical properties. Hence, unless taken into a self-consistent procedure, such an inconsistency renders the MCSCRF model inappropriate for the description of pure liquids. Previously, this problem has been left rather unnoticed, probably due to the molecular focus adopted in many theoretical studies of solvation. The consideration of deriving a macroscopic optical property, such as the refractive index, clearly reveals the problem.

We considered this issue in a study on the refractive index of benzene, using self-consistent reaction field (SCRF) theory, in its equilibrium, linear-response implementation. In that study [40], we introduced the iterative self-consistent reaction field Method (ISCRF), which, in a self-consistent manner, couples successive SCRF computations of the molecular polarizability, $\boldsymbol{\alpha}(\omega)$, to a macroscopic model for the dielectric constant $\epsilon(\omega)$. In another recent study on benzene [71], the Onsager model in concert with equilibrium SCRF polarizabilities, was used to eliminate the explicit reference to the cavity radius, R_{cav}. This procedure relies on determining the unique value of R_{cav}, which, used in the SCRF computation, makes the Onsager expression reproduce the experimental refractive index. A conclusion of this study was that this unique value of R_{cav} depends only on the level of electronic structure theory and the liquid (solute) in question. Thus, this unique value of R_{cav} may be perceived as a "geometrical" parameter characteristic of the solvated molecule.

Here, we are concerned with the generalization of the ISCRF approach to encompass nonequilibrium solvation along with the unique cavity parameter concept. For such a procedure to be attractive, we demand that nonpolar and polar pure liquids can be treated on an equal footing. From the point of view of electronic structure theory, this is far from trivial. The polarization states of polar and nonpolar liquids differ by a whole range of orientationally induced effects, as borne out by the larger values of the static dielectric constant, ϵ_{st}, for polar liquids. Although qualitatively accounted for by classical solvent theory (Onsager type expressions etc.), these orientational polarization effects are not treated at all in schemes based only on electronic structure methods. Only electronic, and to some extent vibrational [58, 72, 73], polarization contributions to the dielectric function can be obtained from electronic structure methods. Therefore, electronic structure-based continuum solvation methods are suited only for the description of pure, nonpolar liquids, unless merged with a model for molecular orientation. The latter is another conclusion drawn from [71].

By restricting the ISCRF procedure to the optical frequency range — to a first approximation — we may circumvent the above limitations. At optical frequencies, orientational and translational polarization effects become inertial, relative to the electron dynamics, and the polarization state is divided into an optical and an inertial contribution. For optical events, only the optical polarization contribution of the solvent may equilibrate to changes in the solute electronic charge distribution. Accordingly, we are at the core of nonequilibrium solvation. Taking this method into a self-consistent procedure with respect

to the optical dielectric constant, ϵ_{op}, we obtain a model for the refractive index, $n(\omega)$, of pure liquids, self-consistent with respect to electronic degrees of freedom and with ϵ_{st} as the only input.

As a critical test of the nonequilibrium ISCRF procedure, in this work, we seek to compute $n(\omega)$ of liquid water in the optically transparent region. We chose water to challenge the method used, because its highly polar and associated liquid state provides difficulties to the theoretical description irrespective of the frequency range considered. Also, we have used water as a benchmark molecule in previous investigations of the continuum solvation model. This has helped to establish a confidence level with regard to the level of electronic structure theory and choice of basis set. Further, basic requirements for the representation of the molecular environment have been established in order for the SCRF model to perform correctly. As a minimum, both the effect of the first solvation shell and the outer solvent must be considered when describing solvation of the water monomer [23, 74, 75]. The first solvation shell is represented as the local tetrameric water configuration surrounding the central monomer as obtained from a C_{2v} idealization of the experimental ice structure [76] where the number of donor and acceptor hydrogen-bond linkages is the same. The outer solvent is modelled by surrounding the resulting supermolecule with a dielectric medium.

Molecular properties in this approach are simply obtained as differences between properties evaluated for the pentameric (monomer + solvation shell) and tetrameric (only the solvation shell) structures. This approach, referred to as the differential shell approach [23, 74], has the advantage that the explicit effects of the first solvent shell can be identified for an extensive molecular property. Also, it eliminates the effects arising due to an insufficient representation of the coupling of the solvent shell with the outer solvent, i.e., the dielectric medium. However, a major drawback is the assumption of additivity for the computed property.

To the extent that diffraction [76] and molecular dynamics studies [77–80] indicate extensive local ice-structure in liquid water, one could argue that the pentamer constitutes one possible conformer of several that are present in liquid water. Such an approach to the molecularity of water has not been probed before using the semi-continuum model and we term this the cluster approach. Obviously, reference to the first solvation shell is lost, but in return, we avoid the inconsistencies pointed out above.

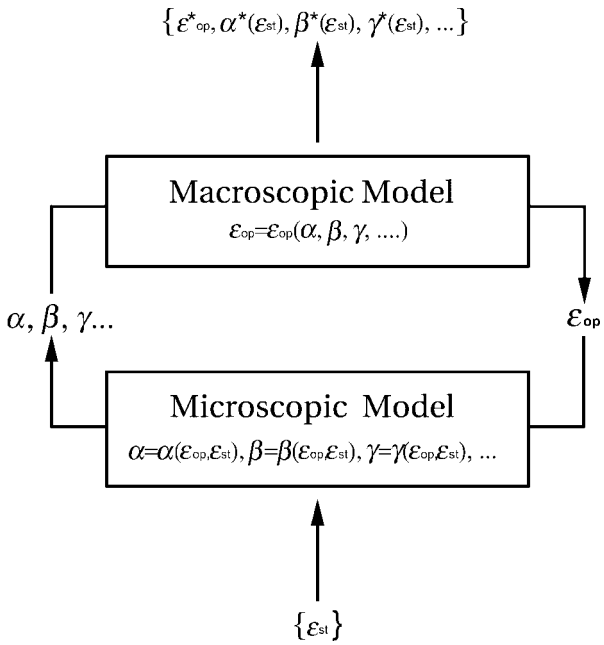

FIGURE 1. Symbolic representation of the ISCRF method. A macroscopic model for ϵ_{op}, in terms of molecular properties, is iteratively coupled to a microscopic model yielding molecular propertied based on ϵ_{op}. For a given density, cavity radius and electronic structure method, ϵ_{st} is the only input for the ISCRF procedure. Converging the iterative process results in a self-consistent set of molecular properties, α^*, β^*, γ^*,...., and optical dielectric constant, ϵ^*_{op}.

2. Theory

In this section, we outline how to obtain the self-consistent determination of molecular optical properties and other macroscopic properties. As illustrated in Figure 1. the basic principle is an iterative coupling of a microscopic and a macroscopic model. By a macroscopic model, we understand some level of classical, macroscopic, electrodynamical theory, which provides expressions for the dielectric function in terms of molecular properties. On the other hand, these properties are determined using a quantum mechanically based microscopic model, which requires the dielectric function as input. The coupling of the microscopic and the macroscopic models constitutes the overall solvent model which we characterize by the functional

$$\boldsymbol{\epsilon}^{(j)} = \boldsymbol{\epsilon}^{(j)}(\alpha, \beta, \gamma, \ldots; N(T)), \tag{1}$$

where $\boldsymbol{\epsilon}^{(j)}$ is the real dielectric tensor, including linear and nonlinear contributions to order j. The

terms $\alpha, \beta, \gamma, \ldots$ symbolize the linear and nonlinear molecular properties.

2.1. THE MICROSCOPIC SOLVATION MODEL

The microscopic model that we use is the nonequilibrium, linear response SCRF model [24]. The cavity shape is spherical with radius, R_{cav}, which reduces the number of arbitrary cavity parameters to a minimum, and the charge distribution of the solute molecule is represented in terms of a multipole expansion. The surrounding dielectric medium is considered linear, isotropic, and homogeneous, and thus only $\epsilon^{(1)}$ is considered. The response of the solvent to changes in the solute charge distribution is approximated as occurring either infinitely slowly or instantaneously. Therefore, the polarization state of the dielectric medium is characterized entirely by an optical, $\mathbf{P}_{\text{op}}$, and an inertial, $\mathbf{P}_{\text{in}}$, polarization vector, and we represent the dielectric medium using the optical dielectric constant, ϵ_{op}, and the static dielectric constant, ϵ_{st}.

The solute sub-system is coupled to the polarization state of the dielectric medium by the Hamiltonian

$$H = H_0 + \tilde{W}_{\text{sol}} + V(t), \tag{2}$$

where $(H_0 + V(t))$ gives the gas phase description of the solute molecule subject to a time dependent perturbing electromagnetic (EM) field. The dependence on the solvent polarization state enters through $\tilde{W}_{\text{sol}}$, due to interaction between $\mathbf{P} = \mathbf{P}_{\text{op}} + \mathbf{P}_{\text{in}}$ and the solute charge distribution. Solving the electronic structure and deriving molecular optical properties for the solute molecule within this model involves the following: (i) An electronic reference state, $|0\rangle$, for the solvated molecule in the absence of the EM field optimized according to the generalized Brillouin condition

$$\langle 0|[\lambda, H_0 + \tilde{W}_{\text{sol}}]|0\rangle = 0, \tag{3}$$

where λ designates the variational parameters. The resulting reference state then defines $\mathbf{P}_{\text{in}}$, which reflects the solvent state before the EM perturbation. (ii) The perturbation, $V(t)$, is applied adiabatically and the solute state propagated according to the Ehrenfest equations of motion using an SCF wave function ansatz. (iii) In propagating the solute state only $\mathbf{P}_{\text{op}}$ is allowed to relax in response to changes in the solute electron distribution, whereas $\mathbf{P}_{\text{in}}$ remains fixed. (iv) Perturbation expansion of time dependent expectations values enables the identification of response functions in terms of Fourier components. The derived response properties for the solute molecule are thus obtained under conditions of nonequilibrium solvation with respect to the inertial polarization field of the solvent.

Restricting the solvent dynamics to either static or instantaneous processes as above naturally limits the model to probing molecules interacting with high-frequency radiation or static fields. At optical frequencies (below the absorption edge) dynamic polarization contributions from molecular vibrations amount to less than ~10% [73], and orientational effects are virtually inertial. Therefore, the microscopic (SCRF) model probes only the electronic solvent dynamics, and consequently, only ϵ_{op} is addressed by the iterative model. On the other hand, ϵ_{st} serves as input, providing an overall, average description of all the inertial solvent degrees of freedom.

2.2. THE MACROSCOPIC MODEL

The macroscopic model is based on the classical electrodynamic treatment of light propagation in continuous media. We consider the medium as an infinite, homogeneous, isotropic, and nonconducting continuum with no free charges. The propagation of EM radiation is then described in terms of the electric, $\mathbf{E}(\mathbf{r}, t)$, and magnetic, $\mathbf{H}(\mathbf{r}, t)$ Maxwell fields, which obey the following wave equations [81]

$$\begin{aligned}
\nabla^2\mathbf{E}(\mathbf{r}, t) &= \frac{1}{c^2}\frac{\partial^2}{\partial t^2}\{\mathbf{E}(\mathbf{r}, t) + 4\pi\mathbf{P}(\mathbf{r}, t)\} \\
&\quad + \frac{4\pi}{c}\frac{\partial}{\partial t}\{\nabla \times \mathbf{M}(\mathbf{r}, t)\}, \\
\nabla^2\mathbf{H}(\mathbf{r}, t) &= \frac{1}{c^2}\frac{\partial^2}{\partial t^2}\{\mathbf{H}(\mathbf{r}, t) + 4\pi\mathbf{M}(\mathbf{r}, t)\} \\
&\quad - \frac{4\pi}{c}\frac{\partial}{\partial t}\{\nabla \times \mathbf{P}(\mathbf{r}, t)\}.
\end{aligned} \tag{4}$$

In Eq. (4), $\mathbf{P}(\mathbf{r}, t)$ and $\mathbf{M}(\mathbf{r}, t)$ designate the macroscopic polarization and magnetization, respectively, and they must be specified according to the constitutive equations in order for Eq. (4) to represent a physical model. Considering linear electric polarization exclusively, we have

$$\mathbf{P}(\mathbf{r}, t) = \chi(\omega)\mathbf{E}(\mathbf{r}, t), \tag{5}$$

where $\chi(\omega)$ is the average linear electric susceptibility. Utilization of the plane-wave solutions in this model leads to the dielectric function

$$\epsilon = (1 + 4\pi\chi). \tag{6}$$

At optical frequencies, it is reasonable to assume additivity in terms of the effective solute polarizability, α^{eff}, to yield the optical susceptibility $\chi_{\text{op}} = N\alpha^{\text{eff}}$, where N is the number density. The optical dielectric constant thus becomes

$$\epsilon_{\text{op}} = n^2 = (1 + 4\pi N\alpha^{\text{eff}}), \tag{7}$$

where α^{eff} is the polarizability as effectively "seen" by the Maxwell field and is not necessarily equal to α^{sol}, the polarizability derived from the solvent computations. Incorporating the effect of molecular interactions into α^{sol}, as described in Section 2.1, requires that $\alpha^{\text{eff}} = f(\omega)\alpha^{\text{sol}}$, where $f(\omega)$ is a local field factor. The explicit form of $f(\omega)$ has been given much attention [82, 83] and is still the subject of some discussion [84]. In the simplest approximation (the Lorentz internal field correction [85]), we have $f(\omega) = \frac{\epsilon_{\text{op}}+2}{3}$, such that Eq. (7) becomes equal to the Clausius-Mossotti (CM) equation

$$\epsilon_{\text{op}} = \frac{(3 + 8\pi N\alpha^{\text{sol}})}{(3 - 4\pi N\alpha^{\text{sol}})}, \tag{8}$$

which, at optical frequencies, is also termed the Lorentz-Lorenz equation.

Although quite approximate, the CM equation has proven surprisingly successful in the description of nonpolar liquids. In fact, Eq. (8) results from the more elaborate Onsager model [86] in the limit of a spherical cavity, treating nonpolar molecules occupying a volume corresponding to

$$\frac{4\pi}{3} N R_{\text{cav}}^3 = 1. \tag{9}$$

Coupling Eq. (8) with the microscopic model may be considered inconsistent, unless R_{cav} is chosen according to Eq. (9) in the SCRF computations. For all practical purposes, this turns out to be impossible. The inconsistency is avoided using the Onsager model [86] where, for a spherical cavity, explicit R_{cav} dependency appears. At optical frequencies where the orientational polarization effects become inertial, we obtain [82]

$$\epsilon_{\text{op}} = \frac{1}{4}\left\{1 + 12\pi N\alpha^{\text{sol}} - \frac{4\alpha^{\text{sol}}}{R_{\text{cav}}^3} + \sqrt{3\left(\left(8 + 48\pi N\alpha^{\text{sol}} - \frac{32\alpha^{\text{sol}}}{R_{\text{cav}}^3}\right)\pi N\alpha^{\text{sol}} + 3\right)}\right\} \times \left\{1 - \frac{\alpha^{\text{sol}}}{R_{\text{cav}}^3}\right\}^{-1}, \tag{10}$$

as an alternative to Eq. (8).

2.3. THE ISCRF PROCEDURE

In the coupling of the SCRF model and a given macroscopic model, self-consistency is required only with respect to ϵ_{op}. Therefore, the resulting polarizabilities are parameterized with respect to ϵ_{st} and R_{cav}

$$\boldsymbol{\alpha} = \boldsymbol{\alpha}(-\omega; \omega : R_{\text{cav}}, \epsilon_{\text{st}}). \tag{11}$$

At a given temperature, ϵ_{st} is fixed, and the iterative coupling gives a self-consistent determination of the set $[\epsilon_{\text{op}}, \alpha]$ parameterized only with respect to R_{cav}. As outlined in Section 2.2, we have three macroscopic models of increasing complexity. Coupling of the SCRF procedure to Eq. (7) or Eq. (8), referred to as the simple and Lorentz schemes, respectively, involves R_{cav} only through the microscopic model. However, coupling to Eq. (10), the Onsager scheme involves R_{cav} explicitly in both models.

Considering R_{cav} as a geometrical parameter characteristic of the solute molecule, level of quantum theory, and the macroscopic model used then allows us to optimize it such that $n^2(\omega) = \epsilon_{\text{op}}$ reproduces the experimental refractive index, n_{exp}.

Despite the dispersive nature of $n(\omega)$, ideally, one should require R_{cav} independent of the optical frequency where the optimization is performed.

3. Computational

Computationally, the microscopic model is realized using the nonequilibrium linear solvent response method, as implemented in the DALTON quantum chemical code [87]. The computations are of semi-continuum nature and as discussed in Section 1, they are performed using either the cluster or the differential shell approach. The latter

TABLE I

Basis set characteristics, polarizabilities for gas phase pentamer, and refractive indices computed for selected contractions and augmentations of the ANO basis set.

			α (au)		n_D	
Basis set	CGTOs	E_{HF} (au)	$\lambda = \infty$	$\lambda = 589$	Equation (7)	Equation (8)
Sadlej	210	−380.2892	42.362	43.046	1.23868	1.28457
ANO[4s3p2d/3s2p]	205	−380.3423	41.975	42.631	1.23660	1.28161
ANO[4s3p2d1f/3s2p1d]	290	−380.3514	42.041	42.699	1.23694	1.28209
ANO[5s4p3d/4s3p]	290	−380.3462	42.329	43.007	1.23849	1.28429
ANO[5s4p3d2f/4s3p2d]	460	−380.3552	42.367	43.046	1.23868	1.28457

requires separate semi-continuum computations for both tetramer and pentamer configurations, whereas for the cluster approach pentamer computations suffice. To compare with results obtained from the traditional use of the macroscopic models, we performed additional gas phase computations for the tetramer and pentamer configurations.

The geometry of the pentamer is identical to the one used previously [23] and possesses the full C_{2v} symmetry characteristic of the central water monomer. The individual water molecules have the molecular geometry: $R_{OH} = 0.958018$ Å and $\theta_{HOH} = 104.500°$. The tetramer is obtained from the pentamer by removal of the central water molecule and thus also has C_{2v} symmetry.

Gas-phase SCF computations were performed for selected decontractions and augmentations of the ANO basis set [88] to find a suitable level of theory, the results of which are collected in Table I. The nomenclature used for the ANO sets designates the degree of decontractions/augmentations on O and H, respectively, relative to the uncontracted polarization set [14s9p4d3f/4s3p2d].

The linear response equations were solved for 13 typical laser frequencies, and in the limit of a static field. The frequency interval ranges from 1064 nm (Nd:YAG) to right below the absorption edge, 193 nm (Argon Fluoride) of liquid water.

The ISCRF procedures are initiated from ϵ_{op}, ϵ_{st} and a cavity radius of 9.00 au. In the first iteration ($q = 1$), ϵ_{op} is derived from either Eq. (7) (simple model), Eq. (8) (CM model), or Eq. (10) (Onsager model) using gas-phase polarizabilities. Note that in the cluster approach polarizabilities for the pentamer are used, whereas in the differential shell approach differences between pentamer and tetramer polarizabilites are used. In subsequent iterations ($q > 1$) ϵ_{op} is derived from the respective polarizabilities from the $(q-1)$th iteration. When polarizabilities computed in successive iterations differ by less than 0.001 au, the ISCRF procedure is considered converged for $R_{cav} = 9.00$ au. Repeating this procedure for gradually smaller values of R_{cav}, allows the determination of a unique R_{cav} for which the converged ϵ_{op} reproduces the refractive index. Because the refractive index is a dispersive quantity, one has to choose a specific frequency for the optimization of R_{cav}. In this study, we "calibrate" the ISCRF procedures at the Sodium D-line (589 nm).

In the cluster approach, we use $N_{pent} = \frac{1}{5}N_{mono} = MW/d$, where MW is the molecular weight and d is the density of water (g/m^3). All ISCRF computations were performed at 298.15 K, where $d = 0.99707$ g/ccm, $\epsilon_{st} = 78.54$ [89], and $n(589\,\text{nm}) = 1.33287$ [90].

4. Results and Discussion

In practical terms, the self-consistent determination of the refractive index involves two steps. First, consecutive ISCRF computations are performed to calibrate a given model. Thereafter, properties at other frequencies are computed using the particular value of R_{cav} and corresponding ϵ_{op}. In the following, we give these steps separate attention, but before doing so we briefly discuss the choice of basis set.

4.1. BASIS SET REQUIREMENTS

The differential shell approach restricts us from treating effects of electron correlation in the MCSCF scheme. However, in the evaluation of α for larger molecules, in practical terms, the neglect of electron correlation to some extent is compensated by an exhausted one-electron space [28, 61]. Therefore, we must ensure that the description of α is saturated with respect to enlargements of the basis set. Computational demands and convergence problems

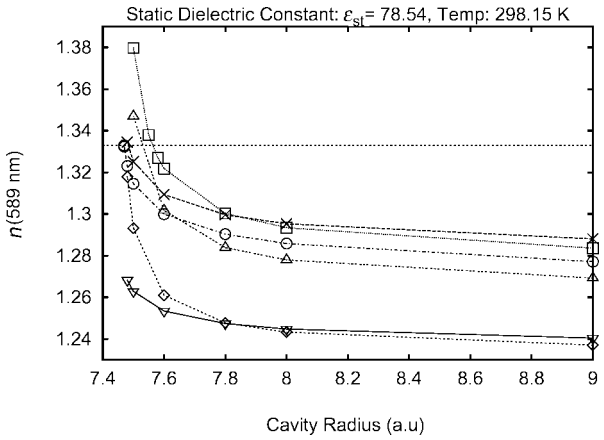

FIGURE 2. The refractive index at 589 nm versus R_{cav}, as obtained in the calibration of the ISCRF procedures using either Eqs. (7), (8) or (10). The horizontal line is the refractive index for the Sodium D-line [62]. Convergence was obtained in the following cases: ($\times$): Clausius-Mossotti/Cluster approach at $R_{cav} = 7.4825$ au, ($\square$): Clausius-Mossotti/Difference shell approach at $R_{cav} = 7.5620$ au, ($\odot$): Onsager/Cluster approach at $R_{cav} = 7.4696$ au, and ($\triangle$): Onsager/Difference shell approach at $R_{cav} = 7.5153$ au. In the simple Lorentz model, neither the cluster (∇) nor the difference shell ($\Diamond$) approach reached convergence.

for the SCRF method for large and diffuse basis sets necessitates a compromise on size.

In Table I, we summarize results for α obtained for the water pentamer with linear-response SCF computations. Only the static and the 589 nm entries are displayed from the set of 14 frequency points computed because, for all frequencies, we observed the same basis set dependence with respect to dispersion. Also, we omit results for the tetramer because these show similar trends.

The smallest basis set is the ANO[432/32], comparable in size with the polarization set due to Sadlej [91] which yields polarizabilities in excess by ~1%. From Table I, we clearly see that the ANO set is unaffected by the further addition of polarization functions. Increasing the diffusiveness by decontraction (ANO[432/32] $\rightarrow$ ANO[543/42]) results in a slight increase of α which is in accord with experience: once the requirements on the polarizable part of the basis are accounted for, residual improvements arise only from addition of diffuse functions [92]. The largest ANO set performs almost identically to the Sadlej set, rendering it an appropriate set. For purposes of calculating the refractive index, the differences in α spanned by different basis sets are quite small as seen from Table I. In fact, variations due to choice of the basis set are insignificant relative to the shift in $n(\omega)$ upon change of solvation model. Overall, we found the ANO[432/32] set the best compromise between size and accuracy for the purpose of this study.

4.2. THE OPTIMIZATION OF R_{cav}

In Figure 2, we display the "stepping" of R_{cav} toward the value, which makes the individual ISCRF procedure reproduce the experimental refractive index (as indicated by the horizontal line). All the calibrations were initiated at $R_{cav} = 9.0$ au, where results are close to the vacuum limit, ($R_{cav} = \infty$), and limited below by $R_{cav} = 7.48$ au. Below this value, penetration of the wave function into the dielectric medium was so extensive that none of the SCRF procedures could be converged. Within these bounds, we were only able to calibrate ISCRF procedures using either the CM or the Onsager model, both within the cluster and differential shell approach. Results for the calibrated cavity radii, for the different ISCRF models, are restated in Table II.

For all three ISCRF procedures, from Figure 2 we see that ${}^{clu}n(\omega) > {}^{diff}n(\omega)$ for large values of R_{cav}. At some point, this order is reversed, starting with the CM model and ending with the Onsager model. As the cavity volume decreases, it is further clear that for all models, it is the differential shell approach which is most susceptible to variations in R_{cav}.

When comparing the curves for the simple model and the CM model, in Figure 2, reveals an almost constant vertical separation. The Onsager model falls in between, with values of ${}^{clu}n(\omega)$ and ${}^{diff}n(\omega)$ slightly smaller than those of the CM model. That the CM model leads to larger values of the polarizability, and thus the refractive index, arises from the fact that Eq. (8) is a special case of Eq. (10), with R_{cav} given as in Eq. (9). With the density used in this study, Eq. (9)

TABLE II

Optimized values of R_{cav} which make different ISCRF procedures reproduce the experimental refractive index, $n_D = 1.33287$, at 298.15 K.

	R_{cav} (au)	
Macroscopic model	Difference	Cluster
Simple Lorentz	—	—
Clausius Mossotti	7.5620	7.4825
Onsager	7.5153	7.4696

The density is 0.99707 g/ccm and the static dielectric constant 78.54.

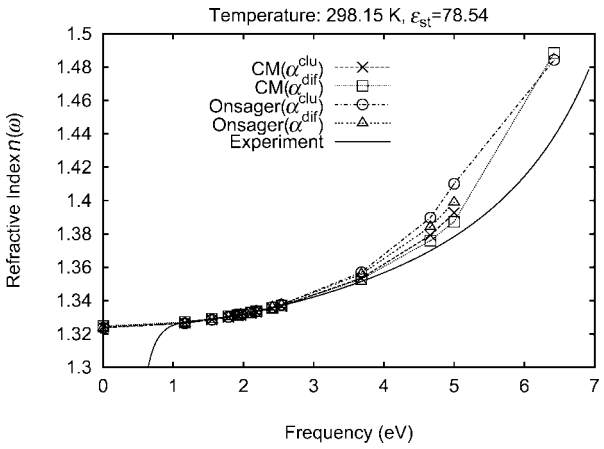

FIGURE 3. Dispersion of the refractive index derived from the four different ISCRF procedures as established in this study at 298.15 K. For the ISCRF(Clausius-Mossotti/cluster) and ISCRF(Onsager/difference shell) approaches, the linear response equations could not be converged for the highest frequency, and the corresponding refractive indices are thus omitted.

corresponds to a cavity radius of 6.229 au, clearly below the range of R_{cav} accessible to the SCRF computations. This inconsistency is a major objection as to the use of the CM model in the ISCRF context.

The failure of the simple Lorentz model to give an ISCRF procedure calibrated to experiment, supports the notion of a field factor, as also emphasized by Wortmann and Bishop [84]. As to the characteristic form of the field factor, ISCRF procedures based on the CM and Onsager models must be tested against each other, the details of which are outlined next.

4.3. THE REFRACTIVE INDEX IN THE ISCRF MODEL

As a first test of the ISCRF procedures, we have computed the refractive index at 298.15 K using either the CM or the Onsager coupling scheme in the iterative procedure. However, a critical test is concerned with the dispersion rather than the absolute magnitude of the refractive index, because the latter comes about through the calibration of R_{cav} in the model. Therefore, it is inherent to the ISCRF procedures that $n(\omega)$ coincides with the experimental result at the calibration frequency, which is also confirmed from Figure 3. Keeping this in mind, we note the excellent description of the dispersion, as provided by the ISCRF procedures in a large part of the frequency range. Below ~1.2 eV, we can obviously not expect the approach to work at all since the explicit vibrational polarization contribution is not accounted for (Fig. 3). At high frequencies, we generally see an exaggeration of the dispersion, being most pronounced for the ISCRF procedures based on the Onsager model. The problem of excessive dispersion is well-known for the macroscopic models used: in the CM case, it is easily perceived as the limiting breakdown of Eq. (8) arising from a vanishing denominator (the CM catastrophe). Especially, for the highest frequency, 193 nm, right below the absorption edge, we additionally encounter problems in converging the linear response equations. For the CM (cluster) and Onsager (differential shell) curves, we have thus omitted the last data point in Figure 3, above 5.0 eV. For these approaches, this indicates that the first-electronic transition may be within the frequency range probed.

Below ~5 eV, the Onsager ISCRF procedures give larger discrepancies relative to experiment as seen from Figure 3. Moreover, within a given model, the differential shell approach performs better. When comparing these trends with the calibrated cavity radii in Table II, we learn that larger values of R_{cav} give rise to a better description of the dispersion. Hence, the ISCRF procedure using the macroscopic model with the largest polarization response gives the best description of the dispersion. From Figure 3, we see that this is achieved with the ISCRF procedure using the CM model in the differential shell approach.

In Figure 4, the dispersion at 298.15 K, obtained for the best performing ISCRF procedure (CM/differential shell), is compared with the corresponding results as derived from Eqs. (7), (8) and (10), using vacuum polarizabilities in the differential shell approach. Clearly, the latter three models yield substantially lower values for $n(\omega)$, getting gradually worse in the order: CM — Onsager — simple Lorentz. The three models display similar dispersions (Fig. 4) which, however, all underestimate the experimetally measured dispersion.

Contrary to what is seen for some nonpolar molecules [82, 93], the use of vacuum polarizabilities in either Eq. (8) or Eq. (10) does not lead to results close to experiment. We emphasize that this is not a direct consequence of neglecting the orientational polarization response in the macroscopic model (because we only probe the optical region).

5. Conclusions

The calculations and model investigations of this study confirm the necessity of using local field

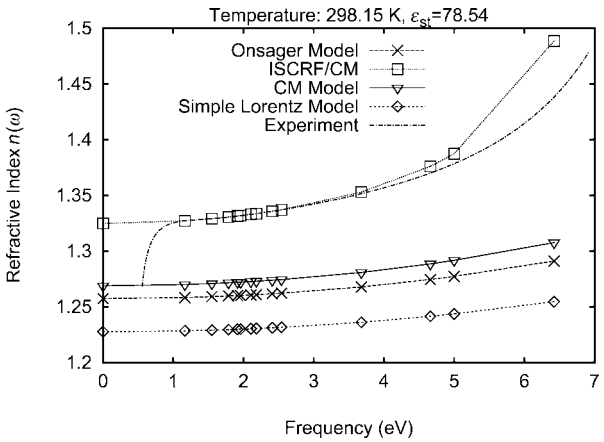

FIGURE 4. Dispersion of the refractive index for the best performing ISCRF (Clausius-Mossotti/difference shell) procedure compared with corresponding results obtained from Eq. (7), (8), and (10) using gas-phase polarizabilities. All of these have been evaluated in the difference shell approach with the ANO[432/32] basis set. For the Onsager model $(\times)$, $R_{cav} = 7.51525$ au, as determined from the corresponding ISCRF procedure, was used in Eq. (10).

factors, the form of which still needs further investigation. For the investigated macroscopic models as based on the assumption of local fields, we observe the best performance for the CM model. However, the differences between the cavity radii as implicitly assumed by the CM model and the corresponding radii used in the SCRF computations, still renders the corresponding ISCRF procedure inconsistent. Nonetheless, the ISCRF procedure based on the CM model gives a very good description of the dispersion of the refractive index of liquid water, in the optical region and at ambient temperature.

By virtue of the calibration procedure, variations in R_{cav} in the macroscopic and microscopic models turn out to be complementary: thus, on increasing the cavity radius in the macroscopic models (e.g., on going from CM to Onsager) will lead to decreases in the cavity radius for the corresponding SCRF procedure.

The solvent models calibrated in this study are general in the sense that, for molecular properties not entering the macroscopic model explicitly (as the magnetic susceptibility), the cavity radii in Table II should be applied directly in SCRF computations of such properties. This in fact constitutes the real test of the ISCRF procedure, along with the calibration of the model at other frequencies, which ideally should leave the model invariant.

We note that the difference shell approach works well, indicating that additivity of polarizabilities holds in this case. As for the cluster approach, it seems that representing liquid water exclusively in terms of pentamer configurations is inappropriate.

References

1. Tomasi, J.; Persico, M. Chem Rev 1994, 94, 2027.
2. Newton, M. D. J Phys Chem 1975, 79, 2795.
3. Noell, J. O.; Morokuma, K. Chem Phys Lett 1975, 36, 465.
4. Beveridge, D. L.; Schnuelle, G. W. J Phys Chem 1975, 79, 2562.
5. Hylton, J.; Christoffersen, R. E.; Hall, G. G. Chem Phys Lett 1974, 24, 501.
6. Contreras, R.; Aizman, A. Int J Quantum Chem 1985, 27, 193.
7. Hoshi, H.; Sakurai, M.; Inone, Y.; Chujo, R. J Chem Phys 1987, 87, 1107.
8. Tapia, O.; In Molecular Interactions; Ratajczak, H.; Orville-Thomas, W. J. Eds.; Wiley: New York, 1980.
9. Warshel, A. Chem Phys Lett 1978, 55, 454.
10. Sanchez-Marcos, E.; Terryn, B.; Rivail, J. L. J Phys Chem 1985, 87, 4695.
11. Rinaldi, D. Comput Chem 1982, 6, 155.
12. Tapia, O. Quantum Theory of Chemical Reactions; Daudel, R.; Pullman, A.; Salem, L.; Veillard, A., Eds.; Wiley: Dordrecht, 1980; Vol. 3, p 25.
13. Karlström, G. J Phys Chem 1989, 93, 4952.
14. Karelson, M.; Zerner, M. J Am Chem Soc 1990, 112, 9405.
15. Day, P. N.; Jensen, J. H.; Gordon, M. S.; Webb, S. P.; Stevens, W. J.; Krauss, M.; Garmer, D.; Basch, H.; Cohen, D. J Chem Phys 1996, 105, 1968.
16. Chen, W.; Gordon, M. S. J Chem Phys 1996, 105, 11081.
17. Cramer, C. J.; Truhlar, D. G. J Am Chem Soc 1991, 113, 8305.
18. Cramer, C. J.; Truhlar, D. G. Science 1992, 256, 213.
19. Mikkelsen, K. V.; Dalgaard, E.; Svanstøm, P. J Phys Chem 1987, 91, 3081.
20. Mikkelsen, K. V.; Ågren, H.; Jensen, H. J. A.; Helgaker, T. J Chem Phys 1988, 89, 3086.
21. Mikkelsen, K. V.; Jørgensen, P.; Jensen, H. J. A. J Chem Phys 1994, 100, 6597.
22. Mikkelsen, K. V.; Luo, Y.; Ågren, H.; Jørgensen, P. J Chem Phys 1994, 100, 8240.
23. Mikkelsen, K. V.; Luo, Y.; Ågren, H.; Jørgensen, P. J Chem Phys 1995, 102, 9362.
24. Mikkelsen, K. V.; Sylvester-Hvid, K. O. J Phys Chem 1996, 100, 9116.
25. Di Bella, S.; Marks, T. J.; Ratner, M. A. J Am Chem Soc 1994, 116, 4440.
26. Yu, J.; Zerner, M. C. J Chem Phys 1994, 100, 7487.
27. Cammi, R.; Cossi, M.; Mennucci, B.; Tomasi, J. J Chem Phys 1996, 105, 10556.
28. Willetts, A.; Rice, J. E. J Chem Phys 1993, 99, 426.
29. Cammi, R.; Cossi, M.; Tomasi, J. J Chem Phys 1996, 104, 4611.

30. Wong, M. W.; Frisch, M. J.; Wiberg, K. B. J Am Chem Soc 1991, 113, 4776.
31. Angyan, J. G. Chem Phys Lett 1995, 241, 51.
32. Olivares del Valle, F. J.; Tomasi, J. Chem Phys 1991, 150, 139.
33. Chipot, C.; Rinaldi, D.; Rivail, J. L. Chem Phys Lett 1991, 191, 287.
34. Cramer, C. J.; Truhlar, D. G. Chem Rev 1999, 99, 2161.
35. Tomasi, J.; Cammi, R.; Mennucci, B. Int J Quantum Chem 1999, 75, 783.
36. Christiansen, O.; Mikkelsen, K. V. J Chem Phys 1999, 110, 1365.
37. Kirkwood, J. G. J Chem Phys 1934, 2, 351.
38. Rivail, J. L.; Rinaldi, D. Chem Phys 1976, 18, 233.
39. Christiansen, O.; Mikkelsen, K. V. J Chem Phys 1999, 110, 8348.
40. Jonsson, D.; Norman, P.; Ågren, H.; Luo, Y.; Sylvester-Hvid, K. O.; Mikkelsen, K. V. J Chem Phys 1998, 109, 6351.
41. Sylvester-Hvid, K. O.; Mikkelsen, K. V.; Jonsson, D.; Norman, P.; Ågren, H. J Chem Phys 1998, 109, 5576.
42. Kongsted, J.; Osted, A.; Mikkelsen, K. V.; Åstrand, P-.O.; Christiansen, O. J Chem Phys 2004, 121, 8435.
43. Aidas, K.; Kongsted, J.; Osted, A.; Mikkelsen, K. V.; Christiansen, O. J Phys Chem A 2005, 109, 8001.
44. Kongsted, J.; Osted, A.; Mikkelsen, K. V.; Christiansen, O. J Phys Chem A 2003, 107, 2578.
45. Kongsted, J.; Osted, A.; Mikkelsen, K. V.; Christiansen, O. J Chem Phys 2003, 118, 1620.
46. Kongsted, J.; Osted, A.; Mikkelsen, K. V.; Christiansen, O. J Chem Phys 2003, 119, 10519.
47. Kongsted, J.; Osted, A.; Mikkelsen, K. V.; Christiansen, O. J Chem Phys 2004, 120, 3787.
48. Kongsted, J.; Osted, A.; Mikkelsen, K. V.; Christiansen, O. Mol Phys 2002, 100, 1813.
49. Osted, A.; Kongsted, J.; Mikkelsen, K. V.; Christiansen, O. J Phys Chem A 2004, 108, 8646.
50. Osted, A.; Kongsted, J.; Mikkelsen, K. V.; Christiansen, O. Mol Phys 2003, 101, 2055.
51. Jensen, L.; van Duijnen, P. T.; Snijders, J. G. J Chem Phys 2003, 118, 514.
52. Jensen, L.; van Duijnen, P. T.; Snijders, J. G. J Chem Phys 2003, 119, 3800.
53. Jensen, L.; Swart, M.; van Duijnen, P. T. J Chem Phys 2005, 122, 034103.
54. Jensen, L.; van Duijnen, P. T. Int J Quantum Chem 2005, 102, 612.
55. van Duijnen, P. T.; de Vries, A. H.; Swart, M.; Grozema, F. J Chem Phys 2002, 117, 8442.
56. Kanis, D. R.; Ratner, M. A.; Marks, T. J. Chem Rev 1994, 94, 195.
57. Willetts, A.; Rice, J. E.; Burland, D. M. J Chem Phys 1992, 97, 7590.
58. Bishop, D. M. Rev Mod Phys page 343, 1990.
59. Bishop, D. M. Adv Quantum Chem 1994, 25, 1.
60. Shelton, D. P.; Rice, J. E. Chem Rev 1994, 94, 195.
61. Kanis, D. R.; Ratner, M. A.; Marks, T. J. Chem Rev 1994, 94, 195.
62. Hammond, B. L.; Rice, J. E. J Chem Phys 1992, 97, 1138.
63. Karna, S. P.; Talapatra, G. B.; Wijekoon, W. M. K. P.; Prasad, P. N. Phys Rev A 1992, 45, 2763.
64. Sekino, H.; Bartlett, R. J. J Chem Phys 1993, 98, 3022.
65. Jonsson, D.; Norman, P.; Luo, Y.; Ågren, H. J Chem Phys 1996, 105, 581.
66. Jonsson, D.; Norman, P.; Ågren, H. J Chem Phys 1996, 105, 6401.
67. Poulsen, T. D.; Ogilby, P. R.; Mikkelsen, K. V. J Chem Phys 2001, 115, 7843.
68. Poulsen, T. D.; Kongsted, J.; Osted, A.; Ogilby, P. R.; Mikkelsen, K. V. J Chem Phys 2001, 115, 2393.
69. Kongsted, J.; Pedersen, T. B.; Strange, M.; Osted, A.; Hansen, A. E.; Mikkelsen, K. V.; Pawlowski, F.; Jørgensen, P.; Hattig, C. Chem Phys Lett 2005, 401, 385.
70. Sylvester-Hvid, K. O.; Mikkelsen, K. V.; Jonsson, D.; Norman, P.; Ågren, H. J Phys Chem A 1999, 103, 8375.
71. Luo, Y.; Norman, P.; Ågren, H.; Sylvester-Hvid, K. O.; Mikkelsen, K. V. Phys Rev E 1998, 57, 4778.
72. Bishop, D. M.; Pipin, J. J Chem Phys, 1995, 103.
73. Luo, Y.; Ågren, H.; Vahtras, O.; Spirko, V.; Jørgensen, P.; Hettema, H. J Chem Phys 1993, 98, 7159.
74. Mikkelsen, K. V.; Ruud, K.; Helgaker, T. Chem Phys Lett 1996, 253, 443.
75. Ruud, K.; Ågren, H.; Rizzo, A.; Coriani, S.; Koch, H.; Sylvester-Hvid, K. O.; Mikkelsen, K. V. J Chem Phys 1997, 108, 599.
76. Narten, A. H. J Chem Phys 1971, 55, 2263.
77. Neumann, M. J Chem Phys 1985, 82, 5663.
78. Neumann, M. J Chem Phys 1986, 85, 1567.
79. Guillot, B. J Chem Phys 1991, 95, 1543.
80. Luzar, A.; Chandler, D.Phys Rev Lett 1996, 76, 928.
81. Wagnière, G. H. Linear and Nonlinear Optical Properties of Molecules; Verlag Helvetica Chimica Acta: Basel, 1993.
82. Böttcher, C. J. F. The Theory of Electric Polarization, Vol. II; Elsevier: Amsterdam, 1984.
83. Böttcher, C. J. F.; Bordewijk, P. The Theory of Electric Polarization, Vol. II; Elsevier: Amsterdam, 1984.
84. Wortmann, R.; Bishop, D. M. J Chem Phys 1998, 108, 1001.
85. Lorenz, L. V. Ann Phys 1880, 11, 70.
86. Onsager, L. J Am Chem Soc 1938, 58, 1486.
87. DALTON. A Molecular Electronic Structure Program, Release 2.0, 2005. Available at: http://www.kjemi.uio.no/software/dalton/dalton.html.
88. Widmark, P.-O.; Malmqvist, P.-Å.; Roos, B. O. Theor Chim Acta 1990, 77, 291.
89. Lide, D. R. Handbook of Chemistry and Physics; CRC Press, Inc.: London, 1973.
90. Thormahlen, I.; Straub, J.; Grigull, U. J Phys Chem Ref Data 1985, 14, 933.
91. Sadlej, A. J. Collect Czechoslov Chem Commun 1988, 53, 1995.
92. Hammond, B. L.; Rice, J. E. J Chem Phys 1992, 97, 1138.
93. Jensen, L.; Schmidt, O. H.; Mikkelsen, K. V.; Astrand, P. O. J Phys Chem B 2000, 104, 10462.